

Figure S1: Annual mean profiles (y axis, height [km]) of cloud frequency (x axis) over the Barbados (between 61.5°W and 49.5°W and 11°N and 19°N) for different satellite datasets (colored lines) and for the Barbados Cloud Observatory (Nuijens et al., 2014) with (solid grey line) and without precipitation (dashed grey line). The dash-dot, dash and solid blue lines correspond to CALIPSO Kyushu University (Cesana et al., 2016), CALIPSO Science Team (Cesana et al., 2016) and CALIPSO-GOCCP (Guzman et al., 2017, same as used in this study) datasets. The solid and dash red lines correspond to CloudSat dataset (Marchand et al., 2008) with and without precipitation (following the definition of Nuijens et al., 2014). The solid and solid-circle green lines correspond to RL-GeoProf dataset with (same as used in this study and Cesana et al., 2019b) and without CF_{lidar} threshold. Finally, the dash-dot and solid purple lines correspond to an older version of the RL-GeoProf dataset using an erroneous lidar product (Kay and Gettelman, 2009) and the 2BCCL dataset using a different Lidar input from the current RL-GeoProf product. Modified from Nuijens et al. (2014).

Cloud Frequency over the Barbados (BCO)

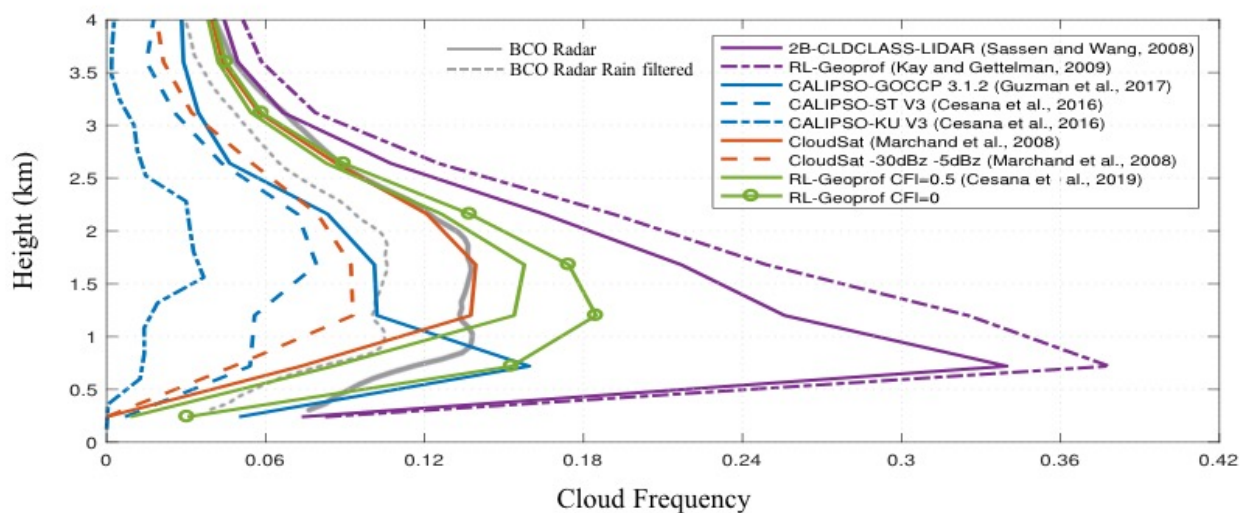
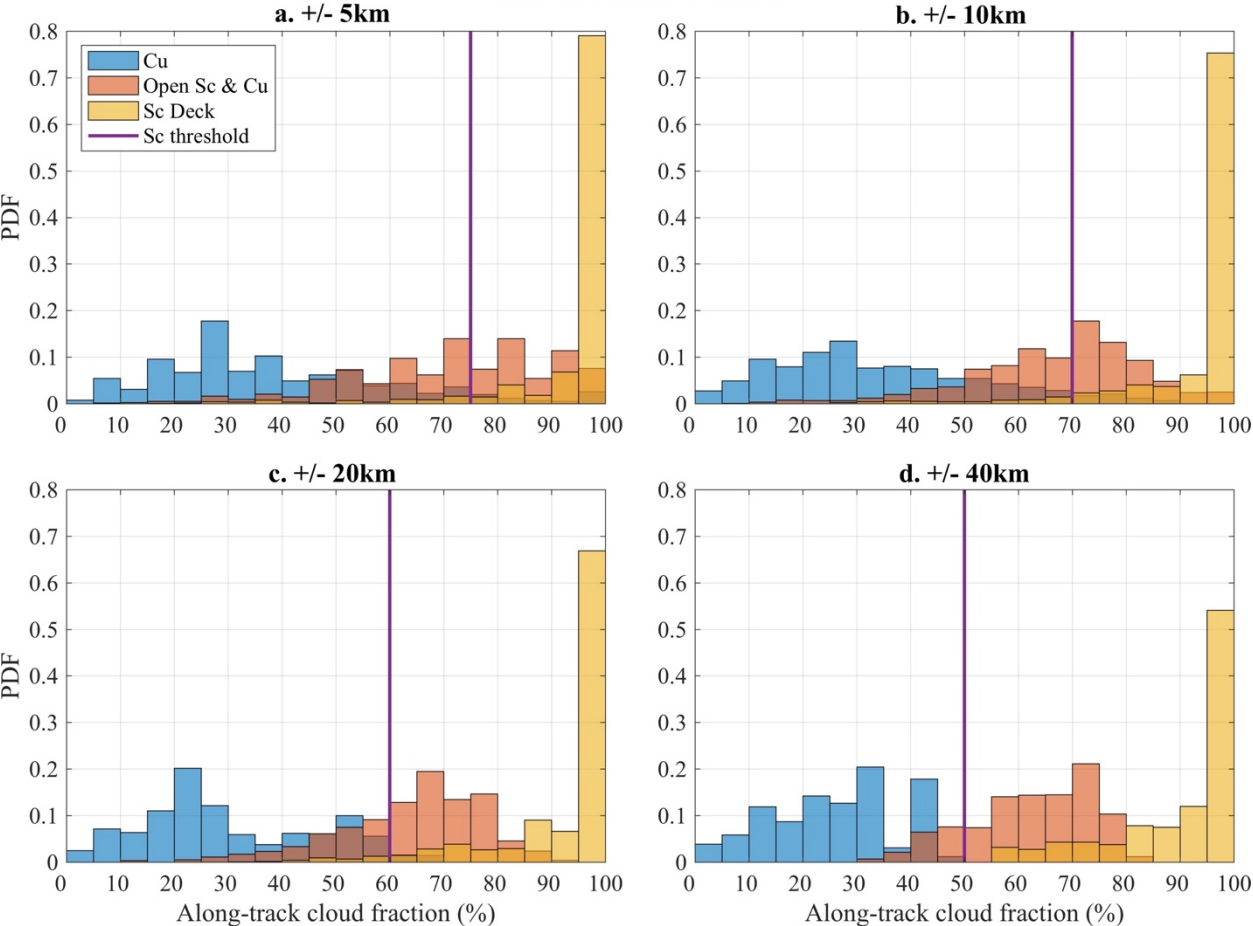


Figure S2: PDF of the different along-track CHCFs for Cu (blue), broken Sc and Sc-Cu transitioning (light red) and Sc (yellow) typical regions computed from eight orbit segments. The thresholds are represented in purple, at approximately the overlap of the Sc and Cu distributions.



5

Figure S3: Map of (x axis, longitude [$^{\circ}$ E]; y axis, latitude [$^{\circ}$ N]) of low-level cloud fraction (%) as observed by CALIPSO-GOCCP (2007-2016). All the orbit segments used in the case study analysis (section 4.1) are represented on the map: stratocumulus off the coast of California (in red), the cumulus in the south-east Pacific and near the Barbados (in blue) and the open-cell Sc and Sc-Cu transitioning case between the south-east Pacific and the Southern Ocean (in grey).

5

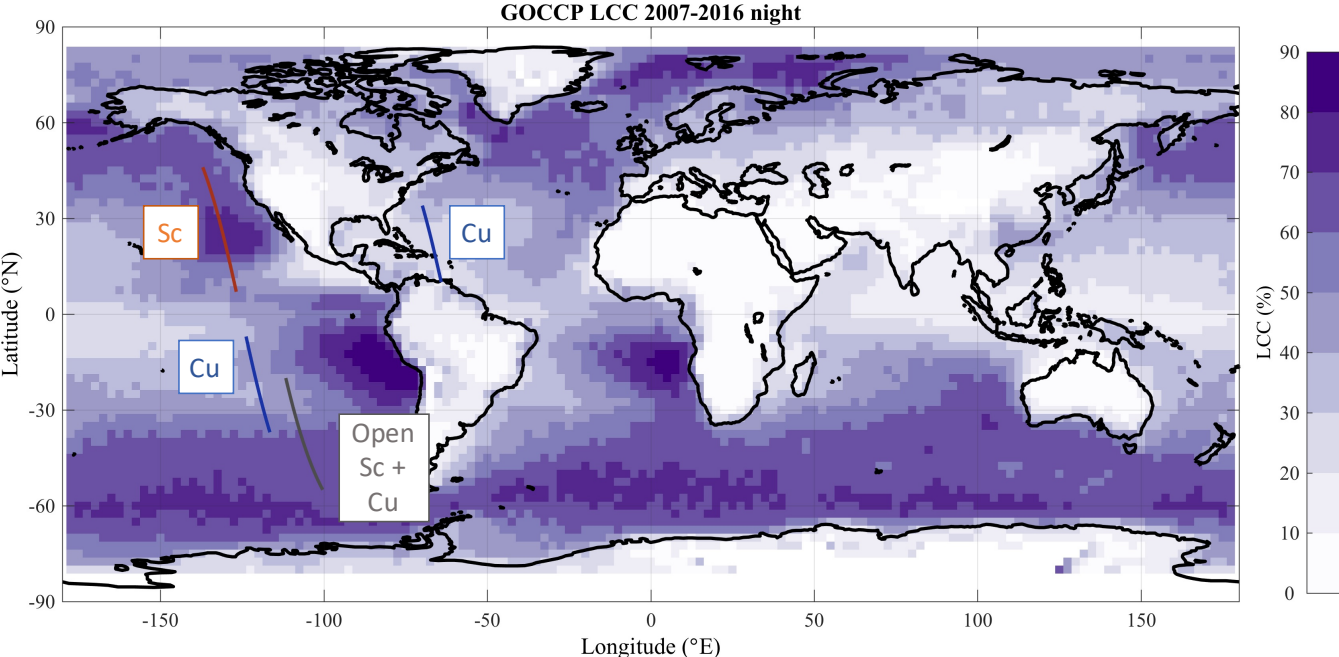


Figure S4: Maps (x axis, longitude [$^{\circ}$ E]; y axis, latitude [$^{\circ}$ N]) of (a) the ratio Sc to Sc-and-Cu cloud (%) for GOCCP Sc-Cu mask, (b) the ratio of opaque to opaque-and-thin cloud (%), as defined in Guzman et al., 2017) and (c) the difference between (b) and (c).

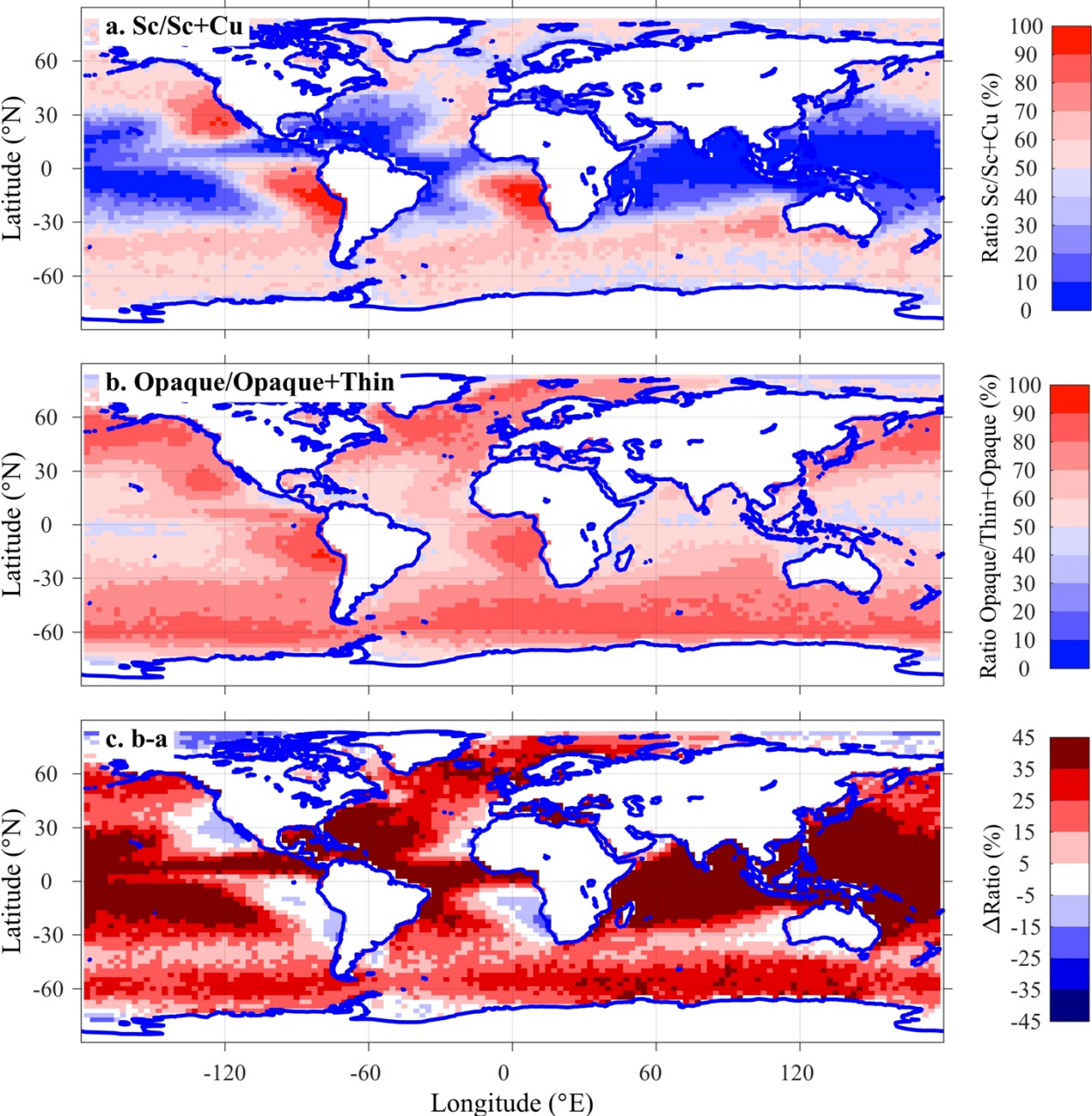
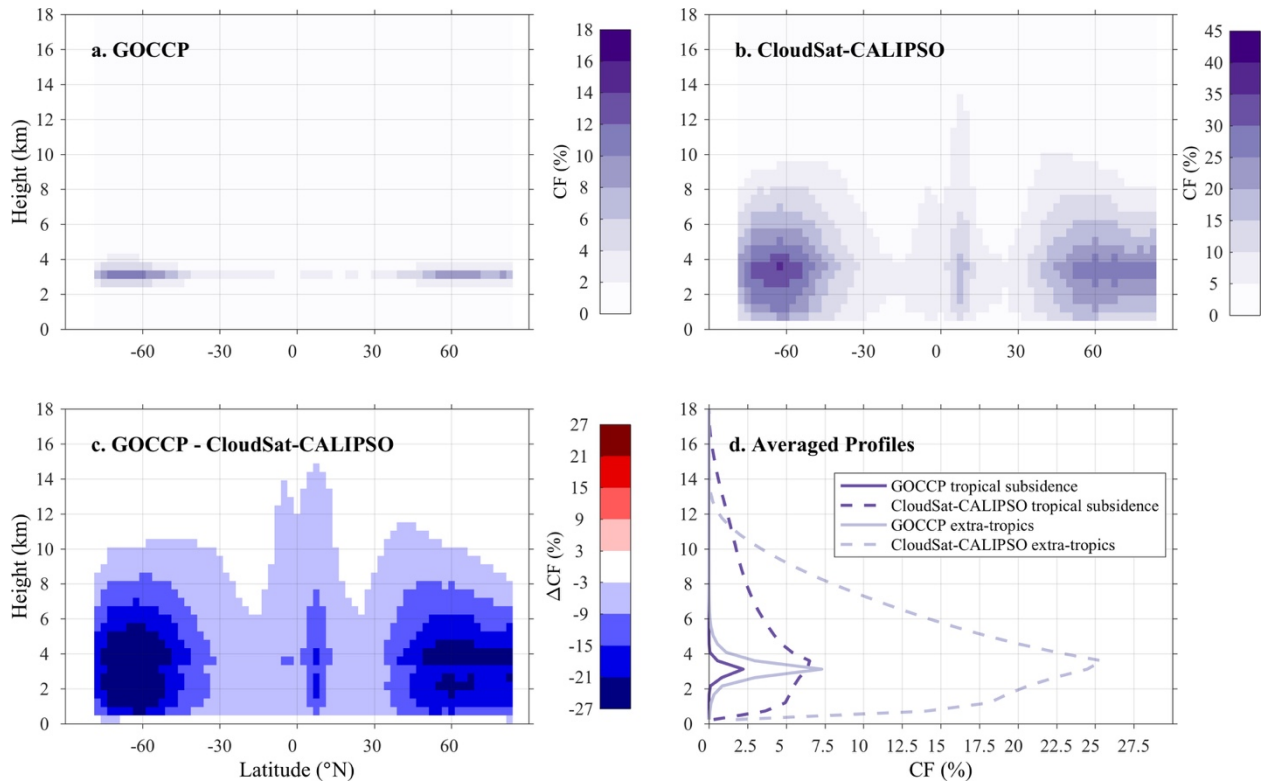


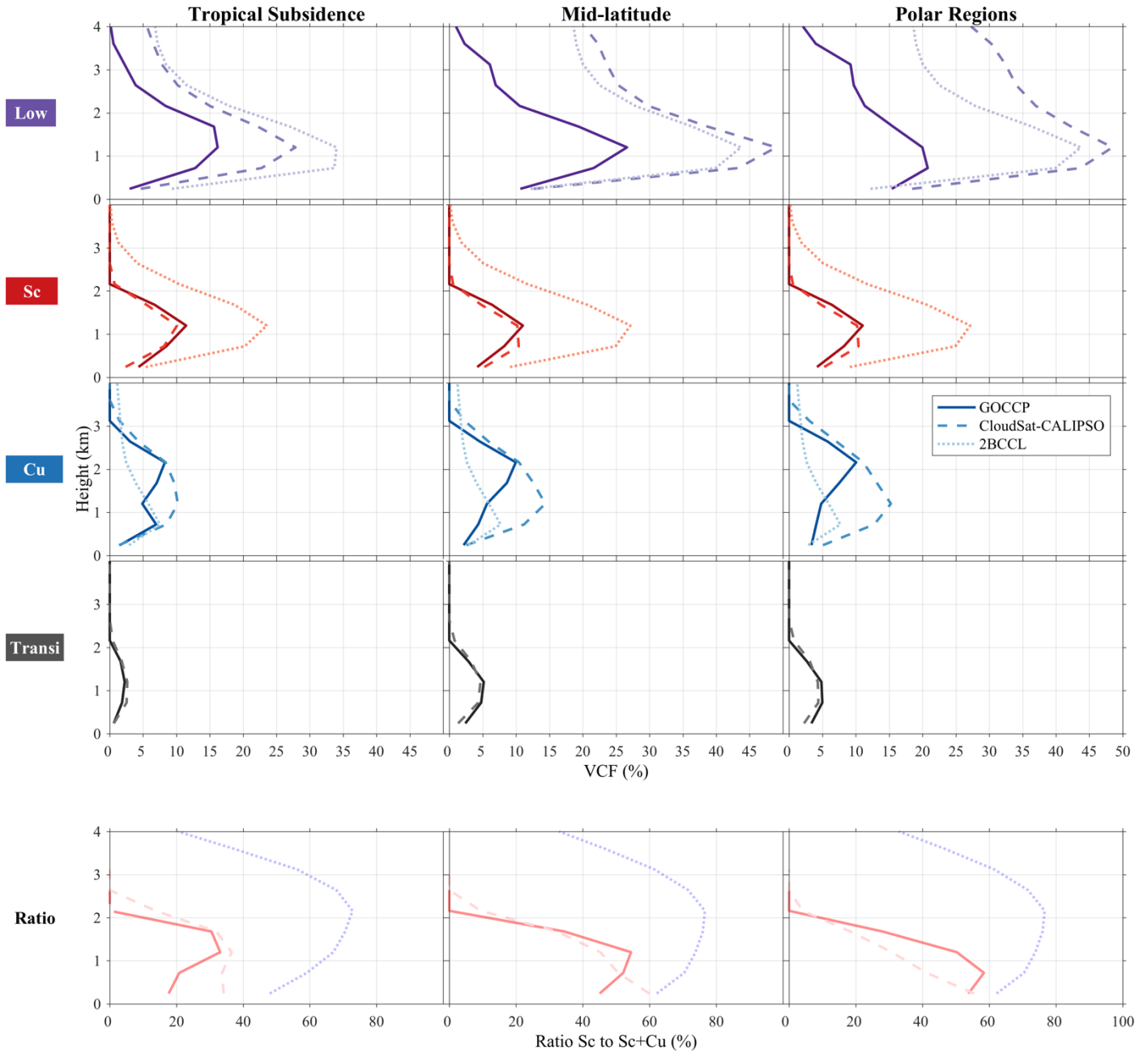
Figure S5: Profiles (y axis, height [km]) of zonally-averaged clouds (x axis, latitude [$^{\circ}$ N]) with a mid- or high-level cloud top and low-level cloud base –i.e., excluding Sc, Cu and Sc-Cu transitioning clouds– for (a) GOCCP, (b) RL-GeoProf and (c) the difference between (a) and (b). The averaged profiles in tropical subsidence regimes ($\omega_{500} > 10$ hPa/day between 35° S/N, solid line) and in the extra-tropics (poleward 35° S/N, dashed lines). The light and dark purple lines in (d) correspond to GOCCP and RL-GeoProf, respectively. In regimes dominated by low clouds, i.e., tropical subsidence regimes, these mid- and high-level topper clouds are very rare and generate only a small difference between GOCCP and RL-GeoProf (d, solid lines) compared to the extra-tropics (d, dashed lines).



10

Figure S6: Profiles (x axis, cloud fraction [%]; y axis, height [km]) of low (first row), Sc (second row), Cu (third row) and Sc-Cu transitioning (fourth row) clouds for (solid line), RL-GeoProf (dashed line) and 2BCCL (dotted line) in tropical subsidence regimes ($\omega_{500} > 10$ hPa/day between 35°S/N, left column same as Fig. 15, fourth column), at mid-latitudes (between 35°S/N to 60°S/N, middle column) and in the polar regions (poleward 60°, right column).

5



6